Dalton Transactions

PAPER

View Article Online
View Journal

Cite this: DOI: 10.1039/c6dt04833a

Intracellular detection of hazardous Cd^{2+} through a fluorescence imaging technique by using a non-toxic coumarin based sensor†

Chanda Kumari,[a] Dibyendu Sain,[a,b] Ashish Kumar,[a] Sushanta Debnath,[c] Partha Saha[c] and Swapan Dey*[a]

Received 22nd December 2016,
Accepted 26th January 2017

DOI: 10.1039/c6dt04833a

rsc.li/dalton

A new coumarin based turn on fluorescent sensor (**R1**) was reported for the detection of highly hazardous **Cd^{2+}** with excellent selectivity and sensitivity without any interference of other metal ions. The single crystal X-ray structure analysis of the sensor showed the actual geometry of the molecule. For the first time, a **Cd^{2+}** induced FRET mechanism was observed and explained accordingly. Instant naked eye detection of **Cd^{2+}** through a sharp colour change signified the practical applicability of **R1**. The sensor of high quantum yield was applied in the intracellular detection of poisonous **Cd^{2+}** in living HeLa S3 cells.

Introduction

Cadmium has adverse power of causing severe environmental and human health problems due to its toxic effect including carcinogenicity.[1] So, it is an enlisted element of seventh rank in the Agency for Toxic Substances and Disease Registry (ATSDR).[2] The level of cadmium accumulation in the environment is increasing dramatically due to various human activities such as mining, metallurgy, smelting, military affairs, fossil fuel combustion, use of phosphate fertilizers in agriculture, production of nickel cadmium rechargeable batteries and other industrial use.[3] All these cadmium sources result in dietary exposure and increasing percentage of cadmium content in our daily food.[4] Biological effects of such cadmium accumulation in our body include calcium metabolism disorders, renal dysfunction, pneumonitis, pulmonary edema, emphysema and even some types of cancers of the kidney, prostate, lung and pancreas.[5] For these toxic effects, the World Health Organization has fixed the limit of cadmium level at 3.0 μg per liter in drinking water.[6] Therefore, the development of rapid and reliable methods for monitoring traces of cadmium in the environment or *in vivo* biological media is a great challenging field with an aspiration of considerable significance.[7,8]

In recent years, fluorescent sensors are considered as an attractive alternative to monitor extremely poisonous metal ions from biological media (*in vivo* or *in vitro*) because of their great potentiality to afford a highly sensitive, selective, and economical online detection method.[9] Among them, turn on fluorescent sensors have great advantages in molecular recognition and materials chemistry.[10] Although a lot of fluorescent sensors have already been reported with some successful applications for sensing Cd^{2+} in living cells, most of them are deficient in selectivity and sensitivity.[11] The heaviest challenge for sensing of Cd^{2+} arises from the interference of other metal ions like Zn^{2+} and Hg^{2+} which exhibit similar spectral and chemical properties.[12] So, the development of a highly specific and selective sensor for Cd^{2+} without interference of other metal ions is still a challenging real time thorny problem for modern researchers.[13]

In recent days, rhodamine and coumarin moieties are frequently used as fluorescent probes for the detection of different metal ions.[14] Generally, coumarin and rhodamine moieties are used as the donor and acceptor respectively for showing the different energy transfer process because a large overlap can be observed between the absorption spectrum of rhodamine and the emission spectrum of coumarin.[15] For a successful Fourier resonance energy transfer (FRET) process, the spectral overlap between the emission of the donor part and the absorption of the acceptor part of the sensor molecule is necessary and the distance between these two parts is also a deciding factor for this process.[16] In continuation of our

[a]*Department of Applied Chemistry, Indian Institute of Technology (ISM), Dhanbad-826004, India. E-mail: dey.s.ac@ismdhanbad.ac.in; Fax: +91 326 2296563; Tel: +91 326 2235607*

[b]*Department of Chemistry, Indian Institute of Engineering Science and Technology, Shibpur, Howrah, West Bengal-711103, India*

[c]*Crystallography and Molecular Biology Division, Saha Institute of Nuclear Physics, 1/AF Bidhannagar, Kolkata 700064, India*

†Electronic supplementary information (ESI) available: ^{1}H, ^{13}C NMR, MS, FTIR spectra; all photo-physical analysis (UV-Vis and fluorescence): quantum yield, LOD, bar diagram, binding constant calculation, and single crystal X-ray analysis of **R1**. CCDC 1524036 for **R1**. For ESI and crystallographic data in CIF or other electronic format see DOI: 10.1039/c6dt04833a

work,[17] we have described here a coumarin linked rhodamine based molecule as a FRET based turn-on fluorescence sensor system for Cd^{2+} with high selectivity and sensitivity in a semi-aqueous environment. According to our knowledge, it is one of the very few previous reports of Cd^{2+} recognition using the FRET based mechanism.[18]

Results and discussion

At first, 7-amino-4-methylcoumarin (compound **3**) was synthesized by using 3-aminophenol and ethylacetoacetate. After that, it was coupled with a rhodamine moiety to obtain the designed sensor **R1** (Scheme 1). The structure of **R1** was characterized by NMR, mass and IR spectroscopic techniques (see the ESI†). The colourless crystal was developed in ethylacetate solvent using a slow evaporation technique. The solid state structure of **R1** was determined by X-ray crystallographic analysis. **R1** was a triclinic system with the *P*1 space group. The solid state ORTEP diagram confirmed that the spirolactam ring was almost perpendicular to the xanthene moiety and the coumarin moiety made an angle of 116° with that ring (Fig. 1). The crystal packing structure showed the molecular arrangement.

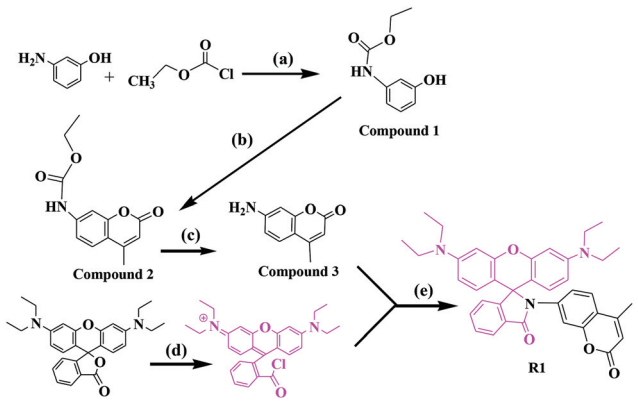

Scheme 1 Reagents and conditions: (a) ethylacetate, rt., 4 h; (b) ethylacetoacetate, 70% H_2SO_4, rt, 4 h; (c) H_2SO_4, acetic acid, 110 °C, 4 h; (d) $POCl_3$, 1,2-dichloroethane, 6 h, reflux; (e) dry Et_3N, dry CH_3CN, 10 h, reflux.

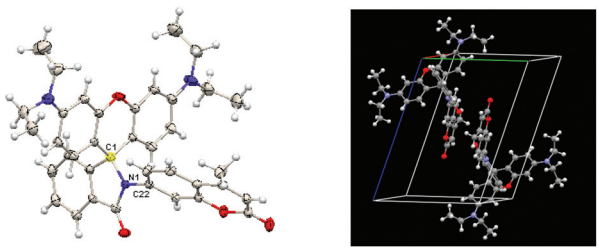

Fig. 1 Single crystal X-ray (a) ORTEP structure of **R1** and its (b) packing structure along the *b* axis.

Complexation studies of R1 with different metal ions through visual detection and UV-Vis spectroscopy

The photo-physical complexation study of **R1** was explored with a series of perchlorate salts of different metal ions such as Li^+, Fe^{3+}, Ni^{2+}, Co^{2+}, Cu^{2+}, Hg^{2+}, Cd^{2+}, Zn^{2+}, Pb^{2+}, and Mg^{2+} in MeOH/H_2O (2/1, v/v, 1 mM HEPES buffer, pH = 7.2) solvent. The colourless solution of **R1** (8.0×10^{-6} M) turned pink immediately upon addition of 1.0 equivalent of Cd^{2+} (8.0×10^{-5} M) (Fig. 2a, inset). In comparison, other cations did not exhibit any changes of **R1**.

The UV-Vis absorbance spectrum of **R1** (8.0×10^{-6} M) in MeOH/H_2O (2/1, v/v, 1 mM HEPES buffer, pH = 7.2) showed no characteristic peak in the visible region, but after gradual addition of Cd^{2+}, a peak at 561 nm was visualized with increasing peak intensity. The spirolactam ring opening by the influence of Cd^{2+} was the main reason behind the visual colour change. Other metal ions were almost inactive towards **R1** and hence they did not show any type of spectral change (Fig. 2b). Moreover, no interference effect of any other metal ions in UV-vis absorption spectra was observed when the solution of **R1** was treated with Cd^{2+} in the presence of other metal ions (Fig. 2b).

The complexation study of **R1** with all the above mentioned metal ions was also carried out using a fluorescence spectroscopic technique. The solution of **R1** (8.0×10^{-6} M) in MeOH/H_2O (2/1, v/v, 1 mM HEPES buffer, pH = 7.2) exhibited the fluorescence emission peak at 430 nm and after addition of Cd^{2+}, a new peak at 589 nm was observed when it was excited at 340 nm. The intensity of that new peak enhanced with the increase in the concentration of Cd^{2+} up to 1.0 equivalent (Fig. 3a). This fluorescence spectral change was also observed visually under long wavelength UV light, where the non-fluorescent solution of **R1** turned to bright red fluorescent immediately in the presence of Cd^{2+} (Fig. 3a, inset). No such spectral or visual fluorescence change and any interference effect were observed for other metal ions (Fig. 3b). So, the above results concluded the strong complexation between **R1** and Cd^{2+}.

The receptor showed a strong binding efficiency towards Cd^{2+}. By using Benesi–Hildebrand linear regression analysis,[19] a high binding constant value ($K_a = 7.8 \times 10^5$ M^{-3}) of **R1** with Cd^{2+} was calculated (see the ESI†). The fluorescence quantum

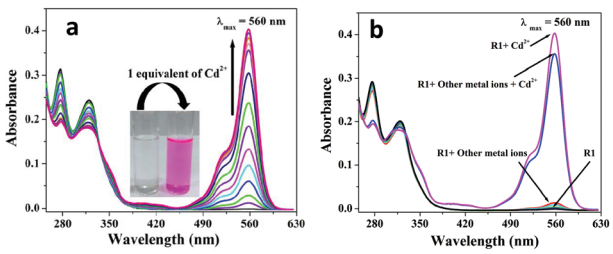

Fig. 2 UV-Vis absorption spectra of **R1** in the presence of (a) 1.0 equivalent Cd^{2+} (inset: colour change of **R1** with Cd^{2+}), (b) other metal ions, in MeOH/H_2O (2/1, v/v), 1 mM HEPES buffer, pH = 7.2.

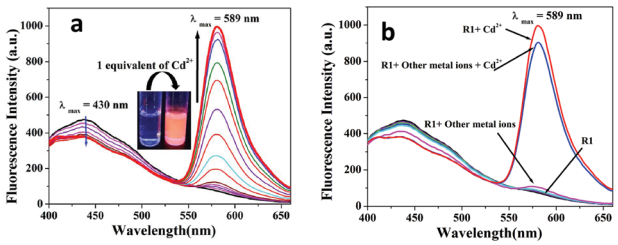

Fig. 3 Fluorescence emission spectra of **R1** (λ_{exc} = 340 nm) in the presence of (a) 1.0 equivalent of Cd^{2+} (inset: visual fluorescence change of **R1** with Cd^{2+}), (b) other metal ions, in MeOH/H_2O (2/1, v/v), 1 mM HEPES buffer, pH = 7.2.

yields[20] (ϕ) for **R1** and **R1 : Cd^{2+}** were found to be 0.011 and 0.19 respectively with respect to standard rhodamine B (literature ϕ = 0.49). The limit of detection (LOD) calculation[21] was carried out using fluorescence titration data. A very low LOD value (1.01×10^{-8} M) obtained by this method implied the high sensitivity of **R1** towards **Cd^{2+}** (see the ESI†).

To investigate the practical applicability, the effect of pH on visual colour change and fluorescence emission of **R1** itself and **R1** with **Hg^{2+}** were examined with a wide range of pH (pH 1.0 to 14.0). **R1** showed pink colour and red fluorescence below pH 6.5, where the spirolactam ring opening form of **R1** persisted. The stability of its ring closure form was found above pH 6.5, where the colourless and non-fluorescence properties were observed. The maximum fluorescence emission intensity of the **R1 : Cd^{2+}** complex was observed at 589 nm in acidic medium (pH 2). The complex exhibited noticeable fluorescence intensity from pH 1.0 to 11.0 suggesting a wide range of practical usability of the sensor (Fig. 4). So the application of **R1** in complexation covered a wide range of pH.

To establish the FRET mechanism, the emission spectra of the donor coumarin moiety (λ_{max} = 430 nm) and the absorption spectra of the acceptor rhodamine moiety (λ_{max} = 555 nm) were merged in a same graph, where a spectral overlap was

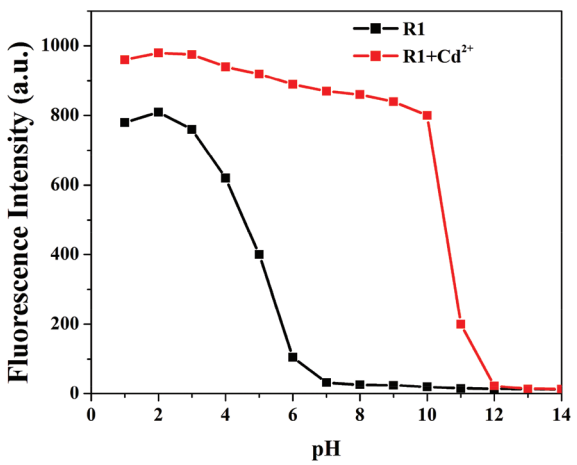

Fig. 4 Influence of pH values on the fluorescence intensities of **R1** and the **R1 : Cd^{2+}** complex at 589 nm.

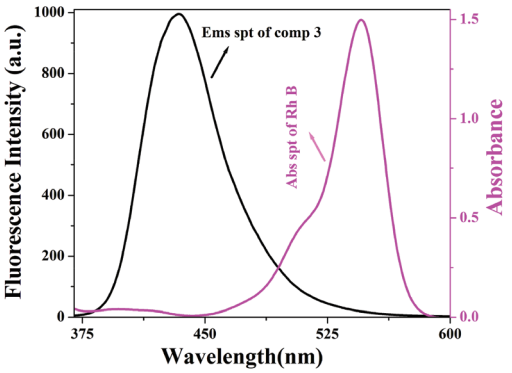

Fig. 5 Overlap plot of absorption spectra of **rhodamine b** and fluorescence emission spectra of compound **3**.

observed (Fig. 5). The spectral overlap confirmed the FRET mechanism for this molecule. In the absence of **Cd^{2+}**, energy transfer between the donor coumarin and the acceptor rhodamine was impossible. But, when **Cd^{2+}** was introduced, the spirolactam ring of the rhodamine moiety opened up through the interaction of **Cd^{2+}** with two 'O' atoms of the coumarin moiety and one 'O' atom of rhodamine. In this way, the whole system of **R1** turned a conjugated system by the influence of **Cd^{2+}** and for this reason the energy of the coumarin moiety transferred easily to the rhodamine moiety *via* 'C=N'. Thus the complexation between **R1** and **Cd^{2+}** was established through the FRET mechanism.

By the test strip experiment,[22] **R1** also displayed its sensing applicability very easily without using any costly instrument to detect **Cd^{2+}**. For this experiment, **R1** coated strips were prepared by dipping the TLC plate in **R1** (3×10^{-5} M) solution. Firstly, **R1** coated strips were colourless but after sinking in **Cd^{2+}** solution, they turned into coloured strips. With the increase in concentration of **Cd^{2+}**, the test strips became more intense pink colour (Fig. 6). So in future, the detection of **Cd^{2+}** could be possible without using any expensive instrument by this method.

Probable binding mode of R1 with Cd^{2+}

A peak of **R1** was found at 600.2794 in mass spectroscopy which was considered as the M + H^+ peak and for the **R1 : Cd^{2+}** complex, it was obtained at 812.6. This value could be assigned for the complex as $[2\mathbf{R1} + 2Cd^{2+} + 2ClO_4^-]^{2+}$. The

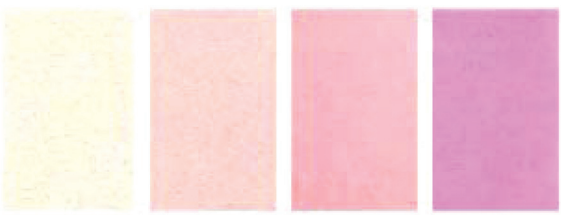

Fig. 6 Images of test strips from left to right: **R1**, **R1** + **Cd^{2+}** (1.5×10^{-3} M), **R1** + **Cd^{2+}** (3×10^{-3} M), **R1** + **Cd^{2+}** (6×10^{-3} M).

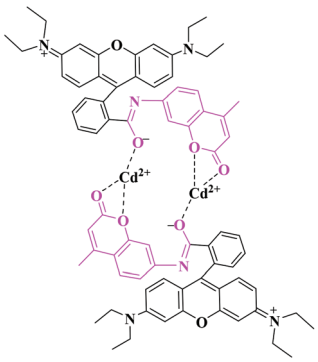

Fig. 7 Probable binding mode of **R1** with Cd^{2+}.

probable binding mode of complexation is shown in Fig. 7, where two Cd^{2+} ions were connected by two **R1** molecules in such a way that each Cd^{2+} was coordinated with two O centers of the coumarin moiety of one **R1** and one O center of the spirolactam moiety of another **R1**. Thus a beautiful cavity was formed by two **R1** molecules for encapsulating two Cd^{2+} ions and this binding mode was also supported by the theoretical DFT calculation.

Fluorescence bio-imaging study

The long wavelength sharp fluorescence emission of the complex was successfully implemented in the intracellular detection of poisonous Cd^{2+} in living HeLa S3 cells, which was the real time most promising practical application of the sensor. To identify Cd^{2+} in living HeLa S3 cells, **R1** was incubated into the cells for half an hour at 37 °C with 5.0 μM 5% EtOH in H_2O in Dulbecco's modified Eagle's medium (DMEM). After that a 5.0 μM solution of Cd^{2+} was inserted into the cell and incubated for another half an hour. Then the cells were processed in a proper way and the fluorescence images were captured. The cells containing only **R1** did not show any fluorescence image in the red channel of a fluorescence microscope (Fig. 8c), but a bright red fluorescence image of the cells incubated with both **R1** and Cd^{2+} was observed (Fig. 8g). This observation concluded that the sensor **R1** could be used as a real time practical kit for detecting Cd^{2+} in living cells and in future this technique can also be applied for *in vivo* detection of Cd^{2+} infected cells in the human body.

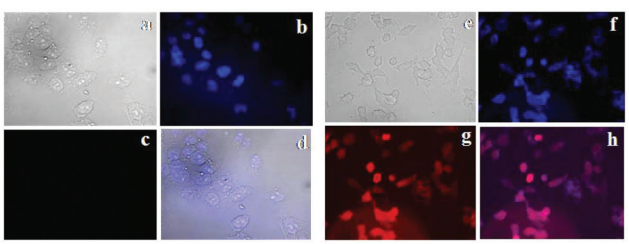

Fig. 8 Fluorescence bio-images of HeLa cells incubated with 5.0 μM **R1** (left side) and the cells incubated with **R1** with 5.0 μM Cd^{2+} (right side): the corresponding bright-field transmission images (a & e); red channel fluorescence images (c & g); blue channel images of DAPI stained cells (b & f); overlay images of red and blue channels (d & h).

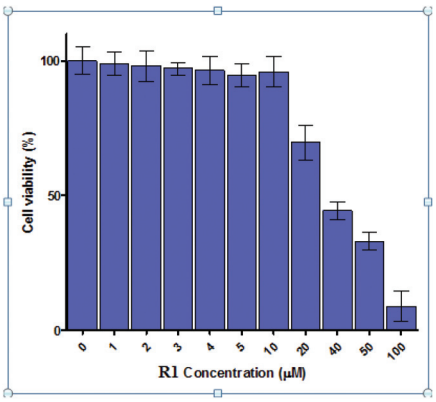

Fig. 9 Checking of viability of cervical cancer cells (HeLa S3 cells) in the presence of **R1**. (Percentage of viability was calculated considering the growth of the HeLa cells without **R1** to be 100%).

Cytotoxicity test

A cytotoxicity test of **R1** was performed to measure its toxicity level and practical applicability in the human body. The test was carried out using the MTT assay of **R1** (Fig. 9). This experiment confirmed that about 90% of these cells remained viable even upon exposure to a 10.0 μM concentration of **R1** for 24 h.

Quantum chemical DFT calculation

For clarification of the binding mode of **R1** with Cd^{2+}, quantum chemical DFT calculation was performed using the Gaussian 09 program with the help of the Gauss-View 5.0 visualization program.[23] The structures were optimized theoretically using the B3LYP/6-311G+(d, p) basis set for **R1** and the B3LYP/LanL2MB basis set for the complex. The energy optimized structure of **R1** suggested that the coumarin moiety was almost perpendicular to the xanthene part of the rhodamine moiety to sustain stability of the system (Fig. 10a) and this structure was also found to be similar to the crystal structure. From the molecular electrostatic potential (MEP) diagram, it was seen that the molecule is mainly divided into two colours, where blue colour was the indication of positive regions and red colour indicated the electronegative regions (Fig. 10b). Electron rich red regions were mainly distributed around the most electronegative centre of the molecule such as N and O atoms. These regions were responsible for easy coordination with the electron deficient Cd^{2+} ion. In the complex structure (Fig. 10c), two **R1** molecules were arranged in such a way that it created a cavity for encapsulating two Cd^{2+} ions by the strong electrostatic attraction with three O atoms for each Cd^{2+}. The optimization energy value of the **R1** : Cd^{2+} complex (−106 639.57 eV) suggested its very high stability compared to **R1** (−52 653.79 eV) (Table 1).

Theoretically calculated energy level diagrams displayed the highest occupied molecular orbital (HOMO) and lowest unoccupied molecular orbital (LUMO) of **R1** and its complex

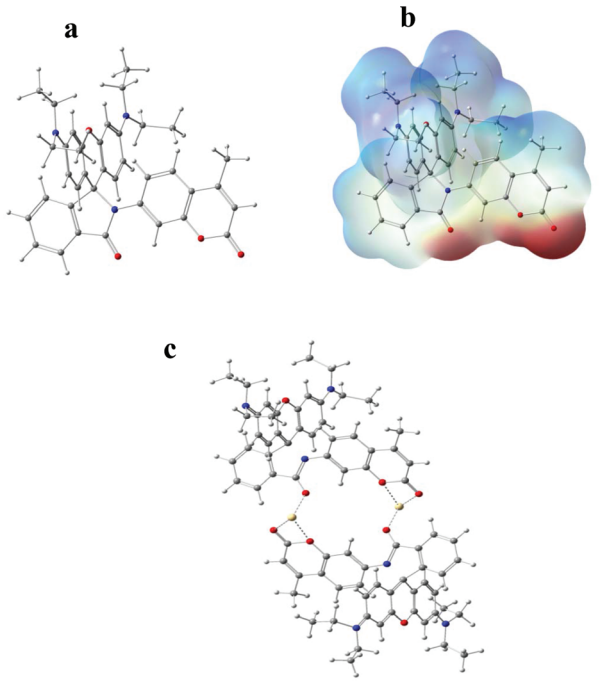

Fig. 10 Optimized structure of (a) **R1** (DFT/B3LYP/6-311G+(d,p) method), (b) MEP map diagram of **R1** and (c) **R1** : Cd^{2+} complex by the DFT/B3LYP/LanL2MB method.

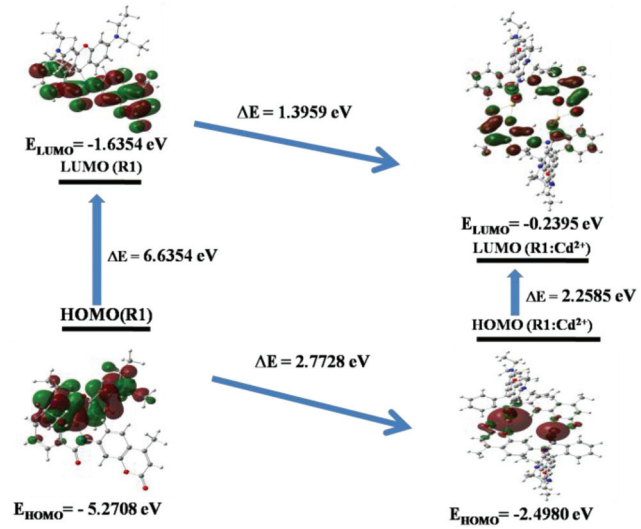

Fig. 11 Energy level HOMO and LUMO diagrams of **R1** and its complex with Cd^{2+}.

along with their spatial distributions. The diagram of **R1** showed that the xanthene moiety contained HOMO orbitals around it whereas coumarin and spirolactam rings contained LUMO orbitals (Fig. 11). On the other hand, HOMO orbitals were mainly situated around the metal ion and LUMO orbitals were placed around the coumarin moiety in the **R1** : Cd^{2+} complex. The corresponding energy values suggested that both the HOMO and LUMO of the **R1** : Cd^{2+} complex were more stable than that of **R1**. It was also observed that the energy gap of HOMO and LUMO orbitals decreased after complexation with Cd^{2+}, which was the preferable condition for complexation of **R1** with Cd^{2+} to show a bathochromic shift in the UV-Vis absorption spectra.[24]

Experimental section

All reagents (AR grade) for synthesis were purchased from Sigma-Aldrich chemicals commercially and used without further purification. All metal perchlorate salts were prepared from the corresponding metal carbonates. Solvents were dried following standard procedures. UV-grade CH_3OH was used for UV-vis and fluorescence titration. ^1H NMR spectra were recorded on a Bruker AV400 instrument using $CDCl_3$ solvent with TMS as an internal standard. ESI-MS measurements were carried out using a microTOF-Q II 10337 mass spectrometer instrument. IR spectra were recorded using a Spectrum 2000 Perkin-Elmer spectrometer. UV–Vis spectra and fluorescence spectra were recorded using a UV-1800 Shimadzu spectrophotometer (1.0 cm quartz cell) and a Perkin-Elmer LS 55 Fluorescence spectrometer, respectively. A Thermo Scientific (FLASH 2000) CHN elemental analyser has been used for elemental analysis. Melting points were determined using a Remco hot-coil stage melting point apparatus and are uncorrected. Fluorescence images of HeLa S3 cells were captured using a Zeiss Axio Observer Z.1 fluorescence microscope.

Cell culture and fluorescence imaging procedure

HeLa cells were grown on cover slips placed in 8 cell cultured disks for 24 hours. Then the cells were treated with **R1** (5.0 μM) for half an hour. The medium containing DMEM, FBS, and PSM (penicillin–streptomycin) was then exchanged with fresh medium. **R1** stained cancer related HeLa cells were then incubated with Cd^{2+} (5.0 μM) for 20 min. After that the cells were washed with saline (1× PBS) and 4% PFA (paraformaldehyde). After 20 minutes, the cells were washed again twice with 1× PBS. The cells were then dried and DAPI was used for staining the cells on the slides. Nail paint was used to seal the cover slips mounted on the glass slides. Images were obtained on a Zeiss Axio Observer Z.1 fluorescence microscope.

Table 1 Optimization energy of **R1** and its complexes with Cd^{2+} calculated using the DFT method

Comp.	Basis set	Optimization energy (eV)	E_{HOMO} (eV)	E_{LUMO} (eV)	$\Delta E_{HOMO-LUMO}$ (eV)
R1	6-311G+(d,p)	−52 653.79	−5.2708	−1.6354	6.6354
R1 : Hg^{2+}	LanL2MB	−106 639.57	−2.4980	−0.2395	2.2585

Cell cytotoxicity assay

The cytotoxicity of **R1** was measured in HeLa cells by the conventional MTT assay.[25] HeLa S3 cells in their exponential growth phase were seeded in 96-well flat-bottom culture plates at a density of 2.6×10^4 cells per well in 100 μl DMEM complete medium (Himedia, India). The cells were allowed to stay and develop for 24 h at 37 °C in a CO_2 incubator (New Brunswick Scientific, USA). The medium was then exchanged with 100 μl fresh medium containing various concentrations of **R1** (0 to 100 μM). The assay was performed in triplicate for each concentration. The cells were then incubated for 24 h, after which the culture medium was removed, and 100 μl of 1 mg ml^{-1} MTT reagent in serum free media was added to each well. After 4 h of incubation, MTT solubilization solution (10% HCl–10% Triton X 100 in anhydrous isopropanol) was added to each well. The resultant solution was calculated spectrophotometrically using a microplate reader at 570 nm and 630 nm. The cytotoxic effect of each treatment was expressed as a percentage of cell viability relative to the untreated control cells. [MTT = (3-(4,5-dimethylthiazol-2-yl)-2,5-diphenyltetrazolium bromide), a yellow tetrazole].

Synthesis of 3-carbethoxyaminophenol (compound 1)

Ethylchloroformate (0.87 mL, 9.16 mmol) was added dropwise in a stirred solution of *m*-aminophenol (1.0 g, 9.16 mmol) in ethylacetate (15 mL) solvent. Instantly, a white precipitate appeared and consequently, the reaction mixture was stirred at room temperature for 2 h. The precipitate of amine hydrochloride was filtered and it was evaporated under reduced pressure to get the colorless crystal of the desired compound.[26]

Characteristic experimental data of compound 1

Melting point: 94–96 °C; **^{1}H NMR (400 MHz, $CDCl_3$):** δ 7.32 (s, 1H), 7.12 (t, J = 8.0 Hz, 1H), 6.64 (d, J = 7.6 Hz, 2H), 6.55 (d, J = 7.6 Hz, 1H), 4.21 (q, J = 7.2 Hz, 2H), 1.30 (t, J = 7.2 Hz, 3H).

Synthesis of 7-carbethoxyamino-4-methylcoumarin (compound 2)

3-Carbethoxyaminophenol (610 mg, 3.15 mmol) was taken in a round bottom flask and ethylacetoacetate (0.48 mL, 13.25 mmol) was added into it. After that, 70% sulfuric acid (9 mL) was added and the reaction mixture was stirred for 4 h at room temperature. After 4 h, the reaction mixture was poured into an ice–water mixture (50 mL). The precipitate was then formed, which was filtered to get 7-carbethoxyamino-4-methylcoumarin.[26]

Characteristic experimental data of compound 2

Melting point: 184–187 °C; **^{1}H NMR (400 MHz, $CDCl_3$):** δ 7.50 (d, J = 8.4 Hz, 1H), 7.42 (d, J = 4.8 Hz, 1H), 7.37 (s, 1H), 6.87 (s, 1H), 6.18 (s, 1H), 4.25 (q, J = 7.2 Hz, 2H), 2.39 (s, 3H), 1.32 (t, J = 7.2 Hz, 3H).

Synthesis of 6-nitro-7-amino-4-methyl-2*H*-chromen-2-one (compound 3)

6-Nitro-7-carbethoxyamino-4-methylcoumarin (1 g, 3.42 mmol) was refluxed in a mixture of conc. H_2SO_4 (4.0 ml) and acetic acid (3.0 ml) for 4 h. After cooling, the mixture was poured into ice water (50 mL). By using NaOH followed by NH_4OH solution, the resulting suspension was made a little basic. Finally, the yellow precipitate was isolated and washed with water to obtain a pure compound.

Characteristic experimental data of compound 3

Melting point: above 250 °C; **^{1}H NMR (400 MHz, $CDCl_3$):** δ 7.34 (d, J = 7.6 Hz, 1H), 6.56 (s, 2H), 6.00 (s, 1H), 4.30 (bs, 2H), 2.33 (s, 3H).

Synthesis of R1

Rhodamine b (125 mg, 0.261 mmol) was taken in dry 1,2-dichloroethane (10.0 ml) and $POCl_3$ was added dropwise into this solution for 15 minutes. Then the reaction mixture was refluxed for 6 h. After removal of the solvent, the reaction mixture was used directly for the next step. Compound **3** (68.96 mg, 0.392 mmol) and Et_3N (1.0 ml) were taken in acetonitrile (6.0 ml) for 10 minutes. Now, this solution was added dropwise to the previous reaction mixture and then refluxed for 8 h. By checking TLC, the completion of the reaction was monitored. After evaporating the solvent under vacuum, the crude residue was purified by column chromatography using 40% EtOAc in pet ether to obtain pure **R1** (solid, white colour, 27% yield).

Characteristic experimental data of R1

Melting point: 275–280 °C; **^{1}H NMR (400 MHz, $CDCl_3$):** δ 7.99 (d, J = 8.0 Hz, 1H), 7.48 (m, 2H), 7.40 (s, 1H), 7.38 (s, 1H), 7.25 (d, J = 2.4 Hz, 1H), 7.11 (d, J = 7.2 Hz, 1H), 7.02 (s, 1H), 6.61 (d, J = 8.8 Hz, 2H), 6.32 (s, 2H), 6.27 (dd, J = 6.4 Hz, 2H), 3.49 (s, 3H), 3.19 (q, J = 7.2 Hz, 8H), 1.15 (t, J = 7.2 Hz, 12H); **^{13}C NMR (100 MHz, $CDCl_3$):** δ 168.4, 161.2, 153.9, 153.7, 152.7, 148.9, 140.8., 133.6, 129.3, 128.2, 124.4, 123.8, 121.5, 117.5, 114.2, 113.2, 108.2, 105.9, 97.8, 67.6, 44.3, 18.5, 12.6; **ESI-MS (+ve mode, *m*/*z*):** found 600.2794 for M + H^+ (Calc. for $C_{38}H_{37}N_3O_4$ is 600.2857); **FT-IR (KBr, cm^{-1}):** 2972 (Ar C–H str.), 1729 (C=O str.), 1698 (amide C=O str.), 1614 (Ar C=C str.), 1265 (aliphatic C–H str.), 1221 (C–N str.), 1119 (C–O–C str.); **Anal. Calcd for R1** ($C_{38}H_{37}N_3O_4$): C, 76.10; H, 6.22; N, 7.01; O, 10.67. Found C, 76.02; H, 6.25; N, 7.00; O, 10.73.

Characteristic experimental data of complexes

ESI-MS (+ve mode, *m*/*z*) of the R1 : Cd^{2+} complex; found 812.13 for $[2\mathbf{R1} + 2Cd^{2+} + 2ClO_4^-]^{2+}$.

Conclusions

In summary, a new coumarin linked rhodamine based sensor was developed for the detection of highly toxic **Cd^{2+}** with superb selectivity and sensitivity. Single crystal X-ray analysis

exhibited the actual structure of the molecule. Instant naked eye detection of Cd^{2+} along with a new absorption peak in the visible region was observed. Probably, this is one of the latest reports of a FRET based turn-on fluorescence sensor system for Cd^{2+}. The nontoxic nature of the molecule in human cells increased its importance to practical life and it was successfully applied in intracellular *in vivo* detection of poisonous Cd^{2+} in living HeLa S3 cells. The probable binding mode and spatial arrangement of **R1** and **R1** : Cd^{2+} complex were calculated by quantum chemical DFT calculation. The detection level of Cd^{2+} was found to be 10.1 nM, hence this molecule could also be used for the detection of excess Cd^{2+} from the environment.

Acknowledgements

CK and AK are thankful to the Indian Institute of Technology (ISM), Dhanbad for providing a Junior Research Fellowship.

Notes and references

1 (*a*) R. A. Goyer, J. Liu and M. P. Waalkes, *BioMetals*, 2004, **17**, 555; (*b*) S. Satarug, J. R. Baker, S. Urbenjapol, M. H. Elkins, P. E. B. Reilly, D. J. Williams and M. R. Moore, *Toxicol. Lett.*, 2003, **137**, 65; (*c*) T. Jin, J. Lu and M. Nordberg, *Neurotoxicology*, 1998, **19**, 529.

2 Agency for Toxic Substances and Disease Registry, 4770 Buford Hwy NE, Atlanta, GA 30341. https://www.atsdr.cdc.gov/spl.

3 (*a*) R. L. Chaney, J. A. Ryan, Y. M. Li and S. L. Brown, *Cadmium in soils and plants*, ed. M. J. McLaughlin and B. R. Singh, Kluwer, Boston, 1999, p. 219; (*b*) N. D. L. Patrick, *Altern. Med. Rev.*, 2003, **8**, 106; (*c*) L. Pari, P. Murugavel, S. L. Sitasawad and K. S. Kumar, *Life Sci.*, 2007, **80**, 650; (*d*) A. M. S. Mendes, G. P. Duda, C. W. A. D. Nascimento and M. O. Silva, *Sci. Agric.*, 2006, **63**, 328; (*e*) F. Beck and P. Ruetchi, *Electrochim. Acta*, 2000, **45**, 2467.

4 L. Friberg, C. G. Elinger and T. Kjellstrom, *Cadmium*, World Health Organization, Geneva, 1992.

5 (*a*) C. D. Klaassen, J. Liu and B. A. Diwan, *Toxicol. Appl. Pharmacol.*, 2009, **238**, 215; (*b*) R. Peng, F. Wang and Y. Sha, *Molecules*, 2007, **12**, 1191; (*c*) M. P. Waalkes, Cadmium carcinogenesis in review, *J. Inorg. Biochem.*, 2000, **79**, 241; (*d*) S. Dobson, Cadmium-Environmental Aspects, *Environ. Health Criter.*, 1992, **135**, 156; (*e*) W. Liu, L. Xu, R. Sheng, P. Wang, H. Li and S. Wu, *Org. Lett.*, 2007, **9**, 3829; (*f*) X. Peng, J. Du, J. Fan, J. Wang, Y. Wu, J. Zhao, S. Sun and T. Xu, *J. Am. Chem. Soc.*, 2007, **129**, 1500.

6 World Health Organization, *Guidelines for drinking water quality*, 3rd edn, 2004, vol. 1, p. 491.

7 (*a*) R. A. Goyer, J. Liu and M. P. Waalkes, *BioMetals*, 2004, **17**, 555; (*b*) S. Satarug and M. R. Moore, *Environ. Health Perspect.*, 2004, **112**, 1099; (*c*) T. Jin, J. Lu and M. Nordberg, *Neurotoxicology*, 1998, **19**, 529; (*d*) M. Nordberg and G. F. Nordberg, *Heavy Metals in the Environment*, ed. B. Sarkar, Marcel Dekker, NY, USA, 2002, ch. 8, p. 231.

8 (*a*) M. Waisberg, P. Joseph and B. Hale, *Toxicology*, 2003, **192**, 95; (*b*) M. P. Waalkes, *J. Inorg. Biochem.*, 2000, **79**, 241; (*c*) M. Mameli, M. C. Aragoni, M. Arca, C. Caltagirone, F. Demartin, G. Farruggia, G. D. Filippo, F. A. Devillanova, A. Garau, F. Isaia, V. Lippolis, S. Murgia, L. Prodi, A. Pintus and N. Zaccheroni, *Chem. – Eur. J.*, 2010, **16**, 919.

9 (*a*) L. Dai, D. Wu, Q. Qiao, W. Yin, J. Yin and Z. Xu, *Chem. Commun.*, 2016, **52**, 2095; (*b*) X. Qian and Z. Xu, *Chem. Soc. Rev.*, 2015, **44**, 4487; (*c*) L. L. Yang, X. M. Liu, K. Liu, H. Liu, F. Y. Zhao, W. J. Ruan, Y. Li, Z. Chang and X. H. Bu, *Talanta*, 2014, **128**, 278; (*d*) W. Cho, H. J. Lee, G. Choi, S. Choi and M. Oh, *J. Am. Chem. Soc.*, 2014, **136**, 1220; (*e*) J. F. Wang, Y. B. Li, N. G. Patel, G. Zhang, D. M. Zhou and Y. Pang, *Chem. Commun.*, 2014, **50**, 12258; (*f*) G. K. Wang, Y. F. Lu, C. L. Yan and Y. Lu, *Sens. Actuators, B*, 2015, **211**, 1; (*g*) X. Liu, D. Mao, J. M. Cole and Z. Xu, *Chem. Commun.*, 2014, **50**, 9329–9332.

10 (*a*) Y. Ding, Y. Tang, W. Zhua and Y. Xie, *Chem. Soc. Rev.*, 2015, **44**, 1101; (*b*) T. Wang, E. F. Douglass Jr., K. J. Fitzgerald and D. A. Spiegel, *J. Am. Chem. Soc.*, 2013, **135**, 12429; (*c*) Y. Xie, P. Wei, X. Li, T. Hong, K. Zhang and H. Furuta, *J. Am. Chem. Soc.*, 2013, **135**, 19119; (*d*) Y. Ding, X. Li, T. Li, W. Zhu and Y. Xie, *J. Org. Chem.*, 2013, **78**, 5328; (*e*) B. Chen, Y. Ding, X. Li, W. Zhu, J. P. Hill, K. Ariga and Y. Xie, *Chem. Commun.*, 2013, **49**, 10136; (*f*) Y. Xie, Y. Ding, X. Li, C. Wang, J. P. Hill, K. Ariga, W. Zhang and W. Zhu, *Chem. Commun.*, 2012, **48**, 11513; (*g*) Y. Ding, Y. Xie, X. Li, J. P. Hill, W. Zhang and W. Zhu, *Chem. Commun.*, 2011, **47**, 5431; (*h*) Y. Ding, W. H. Zhu and Y. Xie, *Chem. Rev.*, DOI: 10.1021/acs.chemrev.6b00021.

11 (*a*) J. Wang, W. Lin and W. Li, *Chem. – Eur. J.*, 2012, **18**, 13629; (*b*) W. Wang, Q. Wen, Y. Zhang, X. Fei, Y. Li, Q. Yang and X. Xu, *Dalton Trans.*, 2013, **42**, 1827; (*c*) W. Ye, S. Wang, X. Meng, Y. Feng, H. Sheng, Z. Shao, M. Zhu and Q. Guo, *Dyes Pigm.*, 2014, **101**, 30; (*d*) Y. M. Zhang, Y. Chen, Z. Q. Li, N. Li and Y. Liu, *Bioorg. Med. Chem.*, 2010, **18**, 1415; (*e*) Z. Shi, Q. Han, L. Yang, H. Yang, X. Tang, W. Dou, Z. Li, Y. Zhang, Y. Shao, L. Guan and W. Liu, *Chem. – Eur. J.*, 2015, **21**, 290; (*f*) X. Y. Liu, D. Y. Liu, J. Qi, Z. G. Cui, H. X. Chang, H. R. He and G. M. Yang, *Tetrahedron Lett.*, 2015, **56**, 1322; (*g*) Z. Liu, C. Zhang, W. He, Z. Yang, X. Gao and Z. Guo, *Chem. Commun.*, 2010, **46**, 6138; (*h*) G. A. M. Jardim, H. D. R. Calado, L. A. Cury and E. N. da Silva Júnior, *Eur. J. Org. Chem.*, 2015, 703; (*i*) Y. Ma, F. Wang, S. Kambam and X. Chen, *Sens. Actuators, B*, 2013, **188**, 1116.

12 (*a*) X. J. Liu, N. Zhang, J. Zhou, T. J. Chang, C. L. Fang and D. H. Shangguan, *Analyst*, 2013, **138**, 901; (*b*) P. X. Li, X. Y. Zhou, R. Y. Huang, L. Z. Yang, X. L. Tang, W. Dou, Q. Q. Zhao and W. S. Liu, *Dalton Trans.*, 2014, **43**, 706; (*c*) J. S. Wu, R. L. Sheng, W. M. Liu, P. F. Wang, H. Y. Zhang and J. J. Ma, *Tetrahedron*, 2012, **68**, 5458; (*d*) E. M. Nolan, J. W. Ryu, J. Jaworski, R. P. Feazell, M. Sheng and

S. J. Lippard, *J. Am. Chem. Soc.*, 2006, **128**, 15517; (*e*) R. Parkesh, T. C. Lee and T. Gunnlaugsson, *Org. Biomol. Chem.*, 2007, **5**, 310; (*f*) G. M. Cockrell, G. Zhang, D. G. VanDerveer, R. P. Thummel and R. D. Hancock, *J. Am. Chem. Soc.*, 2008, **130**, 1420; (*g*) Y. Zhou, Y. Xiao and X. Qian, *Tetrahedron Lett.*, 2008, **49**, 3380; (*h*) S. Banerjee, S. Kar and S. Santra, *Chem. Commun.*, 2008, 3037.

13 (*a*) S. Y. Park, J. H. Yoon, C. S. Hong, R. Souane, J. S. Kim, S. E. Matthews and J. Vicens, *J. Org. Chem.*, 2008, **73**, 8212; (*b*) Y. Wu, H.-Z. Sun, H.-T. Cao, H.-B. Li, G.-G. Shan, Y.-A. Duan, Y. Geng, Z.-M. Su and Y. Liao, *Chem. Commun.*, 2014, **50**, 10986.

14 (*a*) S. Biswas, M. Gangopadhyay, S. Barman and J. Sarkar, *Sens. Actuators, B*, 2016, **222**, 823; (*b*) Y. C. Liu, K. Q. Xiang, M. Guo, B. Z. Tian and J. L. Zhang, *Tetrahedron Lett.*, 2016, **57**, 1451; (*c*) Y. Wang, H.- Q. Chang, W.-N. Wu, X.-L. Zhao, Y. Yang, Z.-Q. Xua, Z.-H. Xuc and L. Jia, *Sens. Actuators, B*, 2017, **239**, 60; (*d*) S. K. Sheet, B. Sen, R. Thounaojam, K. Aguan and S. Khatua, *J. Photochem. Photobiol., A*, 2017, **332**, 101.

15 L. Yuan, W. Y. Lin, B. Chen and Y. N. Xie, *Org. Lett.*, 2012, **14**, 432.

16 (*a*) F. Ge, H. Ye, H. Zhang and B. X. Zhao, *Dyes Pigm.*, 2013, **99**, 661; (*b*) C. Y. Li, Y. Zhou, Y. F. Li, C. X. Zou and X. F. Kong, *Sens. Actuators, B*, 2013, **186**, 360.

17 (*a*) C. Kumari, D. Sain, A. Kumar, H. P. Nayek, S. Debnath, P. Saha and S. Dey, *Sens. Actuators, B*, 2017, **243**, 1181; (*b*) D. Sain, C. Kumari, A. Kumar, H. P. Nayek and S. Dey, *Dalton Trans.*, 2016, **45**, 9187; (*c*) D. Sain, C. Kumari, A. Kumar and S. Dey, *Supramol. Chem.*, 2016, **28**, 239; (*d*) D. Sain, C. Kumari, A. Kumar and S. Dey, *Sens. Actuators, B*, 2015, **221**, 849; (*e*) A. Kumar, D. Sain, C. Kumari and S. Dey, *ChemistrySelect*, 2017, **2**, 1106.

18 K. Aich, S. Goswami, S. Das, C. D. Mukhopadhyay, C. K. Quah and H. K. Fun, *Inorg. Chem.*, 2015, **54**, 7309.

19 (*a*) H. A. Benesi and J. H. Hildebrand, *J. Am. Chem. Soc.*, 1949, **71**, 2703; (*b*) P.-T. Chou, G.-R. We, C.-Y. Wei, C.-C. Cheng, C.-P. Chang and F.-T. Hung, *J. Phys. Chem. B*, 2000, **104**, 7818.

20 (*a*) K. G. Casey and E. L. Quitevis, *J. Phys. Chem.*, 1988, **92**, 6590.

21 (*a*) M. Shortreed, R. Kopelman, M. Kuhn and B. Hoyland, *Anal. Chem.*, 1996, **68**, 1414; (*b*) Y. Yang, T. Cheng, W. Zhu, Y. Xu and X. Qian, *Org. Lett.*, 2011, **13**, 264; (*c*) W. Lin, L. Yuan, Z. Cao, Y. Feng and L. Long, *Chem. – Eur. J.*, 2009, **15**, 5096.

22 (*a*) C. Kumari, D. Sain, A. Kumar, S. Debnath, P. Saha and S. Dey, *RSC Adv.*, 2016, **6**, 62990; (*b*) X. Cheng, Q. Li, C. Li, J. Qin and Z. Li, *Chem. – Eur. J.*, 2011, **17**, 7276.

23 (*a*) M. J. Frisch, *et al.*, *GAUSSIAN 09, Rev. D.01*, Gaussian, Inc., Wallingford, CT, 2009; (*b*) R. D. Dennington II, T. A. Keith and J. M. Millam, *GaussView 5.0*, Gaussian, Inc., Wallingford, CT, 2009.

24 U. Fegade, S. K. Sahoo, A. Singh, P. Mahulikar, S. Attarde, N. Singh and A. Kuwar, *RSC Adv.*, 2014, **4**, 15288.

25 L. V. Rubinstein, R. H. Shoemaker, K. D. Paull, R. M. Simon, S. Tosini, P. Skehan, D. A. Scudiero, A. Monks and M. R. Boyd, *J. Natl. Cancer Inst.*, 1990, **82**, 1113.

26 R. L. Atkins and D. E. Bliss, *J. Org. Chem.*, 1978, **43**, 1975.

